Refractive indices of lithium niobate as a function of temperature, wavelength, and composition: A generalized fit

U. Schlarb and K. Betzler
Fachbereich Physik, Universität Osnabrück, 49069 Osnabrück, Germany
(Received 22 June 1993)

An interferometric method is applied to determine the refractive indices of lithium niobate single crystals over a wide wavelength and composition range. In combination with a careful review of the literature data, a temperature-dependent generalized Sellmeier equation is derived which takes into account the defect structure of Li-deficient $LiNbO_3$. On the basis of this generalized Sellmeier equation, all refractive-index-dependent effects in lithium niobate can be calculated in the wavelength range 400–1200 nm, the composition range 47–50 mol % Li_2O, and the temperature range 50–600 K. The parameters of several optical-characterization methods are computed to state calibration curves in the respective composition range. The calculations of the phase matching conditions for nonlinear effects, such as second-harmonic generation and optical parametric oscillation, show excellent agreement with the respective experimental values.

I. INTRODUCTION

Lithium niobate is a ferroelectric material well known for its technologically important applications. Its interesting electro-optical, nonlinear optical, acoustical, piezoelectrical, and photorefractive properties have been intensively studied.[1–3]

Although commonly referred to as $LiNbO_3$, the material can be fabricated over a relatively wide composition range. The Czochralski technique allows one to grow large-diameter single crystals with solid compositions ranging from about 45 to about 49.5 mol % Li_2O. The highest optical quality and uniformity are achieved at the congruent composition of about 48.38 mol % Li_2O.[4] A recently presented method suggests the addition of potassium to the melt to obtain $LiNbO_3$ crystals of stoichiometric composition.[5,6] Post-growth techniques such as vapor transport equilibration (VTE) also allow one to control the [Li]/[Nb] ratio in the crystal up to a Li content of approximately 50 mol % Li_2O.[7,8]

Controlling the Li content offers the possibility to influence several physical properties; on the other hand the crystal composition has to be checked accurately by appropriate methods. These characterization techniques make use of strongly composition-dependent properties such as the Curie temperature,[9] the optical absorption edge,[10] or the linewidth of lattice modes.[11] The conventional[12] or holographic[13,14] measurement of the birefringence at a fixed wavelength provides a convenient method for the determination of the [Li]/[Nb] ratio. The birefringence between different wavelengths can be measured by nonlinear optical techniques such as second-harmonic generation[15,16] or spontaneous noncolinear frequency doubling.[17]

Since many of these methods rely in some way on the variation of the refractive index with the composition and also certain applications depend on the refractive indices, a precise description of the refractive indices of $LiNbO_3$ is of great interest. Here we present measurements of both the ordinary (n_o) and the extraordinary (n_e) refractive index of $LiNbO_3$ in a composition range from 47 to 50 mol % Li_2O over a wavelength range from 400 to 1200 nm. In contrast to several other authors[8,18,19] who give a description of n_o and n_e only at a fixed composition and in a limited temperature range we propose a relation being a function of the three independent parameters composition, wavelength, and temperature, valid from 50 to 600 K. With this generalized temperature-dependent Sellmeier equation it is possible to derive the parameters and the temperature dependence of all refractive-index-dependent characterization methods.

Moreover, we are able to calculate the conditions for technologically important effects such as second-harmonic generation and optical parametric oscillation.

II. EXPERIMENTAL DETAILS

For the determination of the refractive indices we applied an interferometric technique consisting of a monochromatically illuminated Michelson-type interferometer with a parallel-plate sample in one arm.[20] The sample is rotated around an axis parallel to the c axis of the crystal and perpendicular to the incident beam. In this configuration an increase in the optical path-length difference is caused when the crystal is turned away from normal incidence. This increase can be observed by detecting the shift in the interference pattern at the interferometer output, resulting in a rotation-angle-dependent modulation of the intensity pattern. This interferogram is measured with a computer-controlled setup and is evaluated with appropriate numerical fit procedures, yielding an accuracy in the absolute refractive index of about $\Delta n = 5 \times 10^{-4}$ for samples of good optical quality.[21,22]

Using a helium-neon laser tunable in the visible and infrared region or a mercury vapor lamp combined with a

0163-1829/93/48(21)/15613(8)/$06.00

0.2−m monochromator several wavelengths in the range from 400 to 1200 nm are available. Polarizing the light parallel or perpendicular to the rotation axis makes it possible to measure the extraordinary and the ordinary refractive indices, respectively.

We measured six samples covering a composition range from 46.9 to 49.9 mol% Li_2O. Five crystals grown by the Czochralski technique were characterized by the measurement of the Curie temperature T_C.[23] Applying the relation

$$c_{\mathrm{Li}} = 19.149 + 2.557 \times 10^{-2}\, T_C \tag{1}$$

given by Bordui *et al.*[16] yielded the corresponding Li content. The measurement accuracy for T_C was about 7 °C, resulting in an uncertainty in the composition of less than 0.2 mol%. Spatially resolved second-harmonic generation measurements indicated a homogeneity of the crystals much better than the composition uncertainty.[24,25] One sample was a commercially available vapor transport equilibrated crystal with aproximately 49.9 mol% Li_2O.[8] The typical size after cutting and polishing of the samples was about $8 \times 8 \times 8\mathrm{mm}^3$, well suitable for precise interferometric refractive index measurements.

III. RESULTS AND DISCUSSION

A. Generalized Sellmeier equation

The common way to describe the dispersion of the refractive index is a Sellmeier equation[26]

$$n^2 = 1 + \sum_j \frac{a_j}{\omega_j^2 - \omega^2}\,, \tag{2}$$

where ω_j is the resonance frequency of the jth oscillator and a_j is proportional to the number of oscillators per volume and the transition probability for optical excitation.

For the description of $LiNbO_3$ several oscillator terms have to be taken into account. Since $LiNbO_3$ exists over a wide composition range, these contributions should be more or less dependent on the defect structure. Abrahams and Marsh[27] proposed a model in which each missing Li^+ ion in Li-deficient $LiNbO_3$ is replaced by a Nb^{5+} ion with compensating vacancies at the Nb site maintaining charge neutrality. Defining δ as the ratio of Li sites occupied by Nb^{5+} this can be expressed by

$$[\mathrm{Li}_{1-\delta}]_{\mathrm{Li}}\,[\mathrm{Nb}_{\delta}]_{\mathrm{Li}}\,[\mathrm{Nb}_{1-4\delta/5}]_{\mathrm{Nb}}\,\mathrm{O}_3, \tag{3}$$

with

$$\delta = \frac{10}{3}\,\frac{50 - c_{\mathrm{Li}}}{100}\,, \tag{4}$$

where c_{Li} denotes the Li content of the crystal in mol% Li_2O.

1. *NbO_6 octahedron*

Wiesendanger and Güntherodt showed[28] that the optical anisotropy of $LiNbO_3$ primarily arises from transitions below 7 eV. The optical behavior in this region is governed by the NbO_6 octahedron which determines the lower boundary of the conduction band (d orbitals of Nb^{5+}) and the upper boundary of the valence band (p orbitals of O^{2-}). An oscillator term describing this contribution should be of the form $A_0(\delta)/(\lambda_0^{-2} - \lambda^{-2})$, where $A_0(\delta)$ depends on the composition like $A_0(\delta) = A_0(1 - 4\delta\gamma/5)$. The parameter γ describes how strictly this oscillator depends on the number of Nb on Nb sites ($\gamma = 0$ for no dependence, $\gamma = 1$ for full proportionality).

Our calculations revealed only a minor influence of this parameter on the fit accuracy. This may be explained by the occurrence of ilmenite structured regions in $LiNbO_3$, indicating that vacancies on the Nb or Li site are interchangeable.[29] In order to reduce the number of parameters we therefore chose $\gamma = 3/8$ to obtain

$$\frac{50 + c_{\mathrm{Li}}}{100}\,\frac{A_{0,i}}{\lambda_{0,i}^{-2} - \lambda^{-2}} \tag{5}$$

as the first oscillator term. $i = o$ denotes ordinary, $i = e$ extraordinary polarization.

2. *Nb on Li sites*

The contribution from Nb^{5+} on Li sites can be expressed by an additional oscillator term $A_1(\delta)/(\lambda_1^{-2} - \lambda^{-2})$ with $A_1(\delta)$ depending linearly on the Li site occupancy by Nb. This results in the term

$$\frac{50 - c_{\mathrm{Li}}}{100}\,\frac{A_{1,i}}{\lambda_{1,i}^{-2} - \lambda^{-2}}\,. \tag{6}$$

3. *Temperature dependence*

The two oscillators described are an idealization for the combined density of states of the upper valence band and the lower conduction band regions and the transition probabilities between these states. The same states are responsible for the UV absorption edge of the material. So the temperature dependence of the oscillator frequencies in Eqs. (5) and (6) should behave exactly as the temperature dependence of the UV absorption edge. The latter can be described by the relation proposed by Manoogian *et al.*[30,31] for the temperature variation of the energy gap of semiconductors,

$$\Delta E_{\mathrm{gap}} = UT^s + V\theta\left[\coth\left(\frac{\theta}{2T}\right) - 1\right], \tag{7}$$

where T is given in K and U, s, V, and θ are temperature independent constants characteristic of the respective material. The first term represents the effect of lattice dilatation whereas the coth function arises from electron-phonon interactions. Since the thermal expansion is commonly expressed in terms of a polynomial,[32] we chose $s = 2$ to minimize the number of necessary fit parameters. The temperature dependence of the reso-

nance wavelengths can therefore be expressed by

$$\lambda_{0,i}(T) = \lambda_{0,i} + \mu_{0,i}[f(t) - f(T_0)], \tag{8a}$$
$$\lambda_{1,i}(T) = \lambda_{1,i} + \mu_{1,i}[f(t) - f(T_0)], \tag{8b}$$

with

$$f(T) = (T + 273)^2 + \alpha\left[\coth\left(\frac{\widetilde{T}}{T + 273}\right) - 1\right] \tag{9}$$

and T in °C. $\lambda_{0,i}$ and $\lambda_{1,i}$ are the resonance wavelengths at the reference temperature of $T_0 = 24.5\,°C$. The parameters α and $\widetilde{T}$ can be determined by a fit to the data for the temperature variation of the UV absorption edge from Redfield and Burke[33] and are found to be $\alpha = 4.0238 \times 10^5$ and $\widetilde{T} = 261.6\,°C$. In Fig. 1 the excellent correspondence between experimental data and the fitted curve is shown.

In comparison to the strong variation of the resonance wavelengths the influence of the lattice dilatation on the parameters $A_{0,i}$ and $A_{1,i}$ is negligible. Assuming the corresponding transition matrix elements to be independent of temperature allows one to treat these parameters as constants with no temperature variation.

4. Plasmons

Contributions to the refractive index from the far UV are mainly due to plasmons with energies from 13 to 25.5 eV.[34] With $\lambda_2^2 << \lambda^2$ the corresponding oscillator term can therefore be approximated by $A_2/(\lambda_2^{-2} - \lambda^{-2}) \approx A_2\lambda_2^2$. The plasma frequency is proportional to $\sqrt{N}$ where N is the number of oscillators per volume. Since A_2 is proportional to N, the expression $A_2\lambda_2^2$ is independent of N and is therefore assumed to be independent of composition and temperature. Furthermore, reflectivity measurements[28] show that the optical anisotropy is mainly due to transitions below 7 eV, which allows us to choose the term

$$A_{\mathrm{UV}} = 1 + A_2\lambda_2^2, \tag{10}$$

equal for both polarizations.

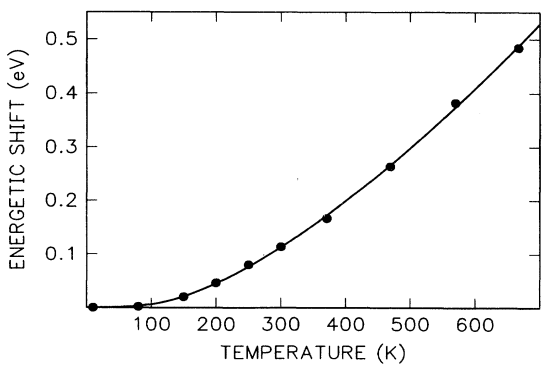

FIG. 1. Temperature variation of the energy gap of $LiNbO_3$ according to Redfield and Burke (Ref. 33). The curve is a fit to these data with the expression proposed by Manoogian and Wooley (Ref. 30).

5. IR term

Contributions from the IR region are supposed to arise from Reststrahl absorption.[35] The large resonance wavelength $\lambda_3^2 >> \lambda^2$ allows one to approximate $A_3/(\lambda_3^{-2} - \lambda^{-2}) \approx -A_3\lambda^2$. Because of its comparatively small influence on the refractive index, A_3 is assumed to be independent of composition and temperature but still polarization dependent. This leads to

$$-A_{\mathrm{IR},i}\lambda^2 \tag{11}$$

as the IR oscillator term.

The final form of the generalized Sellmeier equation is now

$$n_i^2 = \frac{50 + c_{\mathrm{Li}}}{100}\frac{A_{0,i}}{(\lambda_{0,i} + \mu_{0,i}F)^{-2} - \lambda^{-2}} + \frac{50 - c_{\mathrm{Li}}}{100}\frac{A_{1,i}}{(\lambda_{1,i} + \mu_{1,i}F)^{-2} - \lambda^{-2}} - A_{\mathrm{IR},i}\lambda^2 + A_{\mathrm{UV}}, \tag{12}$$

with

$$F = f(T) - f(T_0),$$
$$f(T) = (T + 273)^2 + 4.0238 \times 10^5\left[\coth\left(\frac{261.6}{T + 273}\right) - 1\right],$$
c_{Li} in mol % Li_2O, λ in nm,
T in °C, $T_0 = 24.5\,°C$, $i = e, o$.

The room temperature parameters $\lambda_{0,i}$, $\lambda_{1,i}$, $A_{0,i}$, $A_{1,i}$, $A_{\mathrm{IR},i}$, and A_{UV} are fitted to our measured refractive index data. The measured data for the extraordinary refractive index and the respective Sellmeier fits are shown in Fig. 2. The standard deviation is about 1.3×10^{-3}. The coefficients for the temperature dependence of the refractive indexes $\mu_{0,i}$ and $\mu_{1,i}$ are obtained by a fit to temperature-dependent literature data for congruent[18] and stoichiometric[8] $LiNbO_3$. The numerical results for all parameters are given in Table I.

B. Characterization methods

Many optical-characterization techniques depend in some manner on the refractive indices of $LiNbO_3$. The generalized Sellmeier equation allows one now to calculate the calibration curves for these methods.

One of the earliest methods is the determination of the birefringence at a fixed wavelength and temperature. With the Sellmeier equation a simple general relation can be derived. The temperature variation of the refractive index,

$$n_i^2(c_{\mathrm{Li}}, \lambda, T) = n_i^2(c_{\mathrm{Li}}, \lambda, T_0) + \left.\frac{\partial n_i^2}{\partial F}\right|_{F=0} F, \tag{13}$$

can be approximated with $\coth x \approx 1/x$ to

$$F \approx (T + T_s)^2 - (T_0 + T_s)^2\,, \tag{14}$$

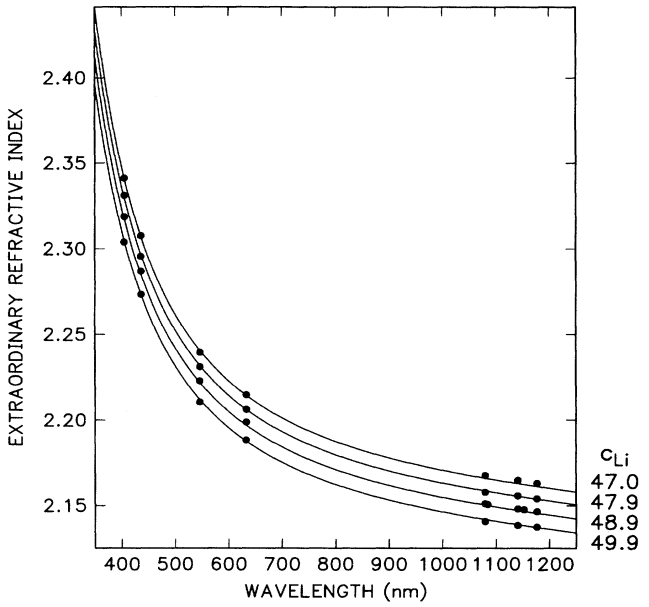

FIG. 2. Dispersion of the extraordinary refractive index of $LiNbO_3$ for several crystal compositions. The curves are calculated from the generalized Sellmeier equation (see text) for $T = 24.5\,^{\circ}\mathrm{C}$.

where $T_s = 273 + \frac{1}{2}\alpha/\widetilde{T} = 1042.1\,^{\circ}\mathrm{C}$. Defining

$$\alpha_i = A_{\mathrm{UV}} - A_{\mathrm{IR},i}\lambda^2, + \frac{A_{0,i}}{\lambda_{0,i}^{-2} - \lambda^{-2}}, \tag{15a}$$

$$\beta_i = \frac{A_{1,i}}{\lambda_{1,i}^{-2} - \lambda^{-2}} - \frac{A_{0,i}}{\lambda_{0,i}^{-2} - \lambda^{-2}}, \tag{15b}$$

$$\gamma_i = \left.\frac{\partial n_i^2}{\partial F}\right|_{F=0} \approx \left.\frac{\partial}{\partial F}\frac{A_{0,i}}{(\lambda_{0,i} + \mu_{0,i}F)^{-2} - \lambda^{-2}}\right|_{F=0} \tag{15c}$$

yields the approximation for the refractive index,

$$n_i = \sqrt{\alpha_i + \frac{50 - c_{\mathrm{Li}}}{100}\beta_i + \gamma_i F} \approx \sqrt{\alpha_i} + \frac{50 - c_{\mathrm{Li}}}{100}\frac{\beta_i}{2\sqrt{\alpha_i}} + \frac{\gamma_i}{2\sqrt{\alpha_i}}F. \tag{16}$$

TABLE I. Parameters of the generalized Sellmeier equation. For the definition see Eq. (12) in the text.

n_o	n_e
$A_{0,o} = 4.5312 \times 10^{-5}$	$A_{0,e} = 3.9466 \times 10^{-5}$
$\lambda_{0,o} = 223.219$	$\lambda_{0,e} = 218.203$
$A_{1,o} = 2.7322 \times 10^{-5}$	$A_{1,e} = 8.3140 \times 10^{-5}$
$\lambda_{1,o} = 260.26$	$\lambda_{1,e} = 250.847$
$A_{\mathrm{IR},o} = 3.6340 \times 10^{-8}$	$A_{\mathrm{IR},e} = 3.0998 \times 10^{-8}$
$A_{\mathrm{UV}} = 2.6613$	$A_{\mathrm{UV}} = 2.6613$
$\mu_{0,o} = 2.1203 \times 10^{-6}$	$\mu_{0,e} = 7.5187 \times 10^{-6}$
$\mu_{1,o} = -1.8275 \times 10^{-4}$	$\mu_{1,e} = -3.8043 \times 10^{-5}$

The birefringence can therefore be expressed as

$$\Delta n(c_{\mathrm{Li}}, \lambda, T) = [c_{\mathrm{Li}} - a(\lambda) - c(\lambda)F]/b(\lambda), \tag{17}$$

where

$$a(\lambda) = 50 - (\sqrt{\alpha_e} - \sqrt{\alpha_o})b(\lambda), \tag{18a}$$

$$b(\lambda) = -100\left(\frac{\beta_e}{2\sqrt{\alpha_e}} - \frac{\beta_o}{2\sqrt{\alpha_o}}\right)^{-1}, \tag{18b}$$

$$c(\lambda) = -b(\lambda)\left(\frac{\gamma_e}{2\sqrt{\alpha_e}} - \frac{\gamma_o}{2\sqrt{\alpha_o}}\right). \tag{18c}$$

Transposing Eq. (17) to

$$c_{\mathrm{Li}} = a(\lambda) + b(\lambda)\Delta n + c(\lambda)\left[(T + T_s)^2 - (T_0 + T_s)^2\right], \; T \text{ in } ^{\circ}\mathrm{C}, \tag{19}$$

makes it possible to determine the composition of an unknown crystal by the measurement of the birefringence at any given wavelength and temperature. In Fig. 3 several calibration curves are computed and compared with our experimental data and results from other authors. The comparison indicates that the relation stated above holds in a temperature range from 0 °C to at least 400 °C and a wavelength range from 400 to 1200 nm. The wavelength dependence of the parameters $a(\lambda)$, $b(\lambda)$, and $c(\lambda)$ is depicted in Fig. 4.

Another method to determine the birefringence is anisotropic holographic diffraction.[14,13] More directly accessible is the measurement of diffraction angles. The parameters for both techniques can be derived from the given Sellmeier equation, too.[36]

Földváry *et al.*[10,37] proposed the position of the optical absorption edge as a sensitive measure for the stoichiometry of $LiNbO_3$ single crystals. In combination with a Kramers-Kronig analysis the shift of the optical absorption edge with composition can be computed with rather high

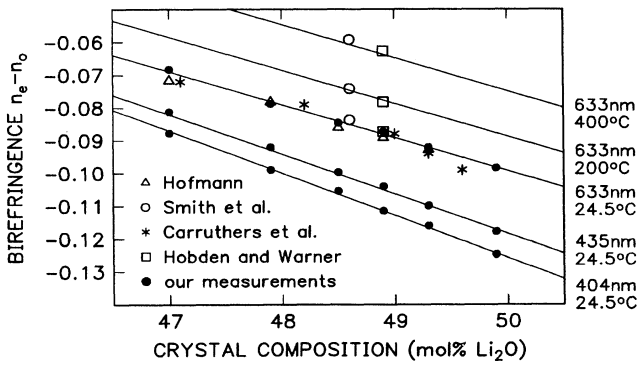

FIG. 3. The birefringence of $LiNbO_3$ as a function of the Li content for various wavelengths and temperatures. The linear relations are derived from the generalized Sellmeier equation. Data points represent our measurements and results from other authors (Refs. 9, 12, 19, and 35). The crystal compositions for Refs. 12 and 35 are determined from the Curie temperatures given in the original papers according to Eq. (1).

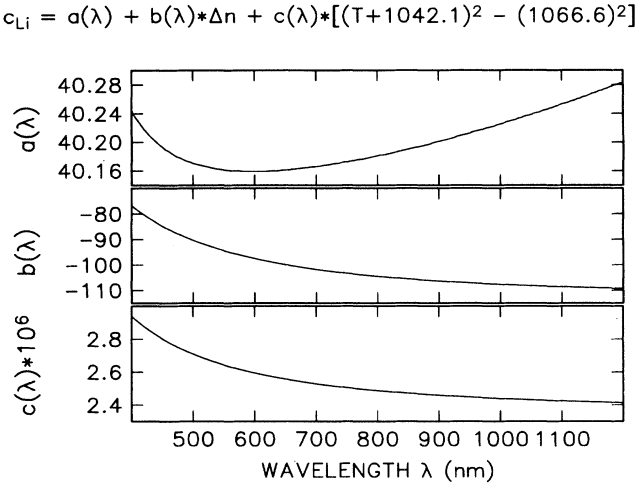

FIG. 4. Wavelength dependence of the birefringence parameters a, b, and c (see text) for $LiNbO_3$.

accuracy from the generalized Sellmeier equation.[36]

Several nonlinear techniques have been proposed for the determination of the Li content in $LiNbO_3$. They all utilize the birefringence between different wavelengths or its variation with temperature. But as nonlinear effects are also of great technological interest (for example, "warm" phase matching of 1064 nm radiation in stoichiometric $LiNbO_3$) they are discussed separately in the following section.

C. Nonlinear effects

The phase matching parameters of all nonlinear effects can be calculated from the conditions for energy and momentum conservation,

$$\sum_i \omega_i = 0, \tag{20a}$$

$$\sum_i \vec{k}_i = 0\ , \tag{20b}$$

where the indices i refer to the interacting beams. Here we will concentrate on second-order effects such as second-harmonic generation and difference frequency mixing, where three beams interact.

1. Noncollinear frequency doubling

In the technique of spontaneous noncollinear frequency doubling first presented by Giordmaine[38] the vectorial phase matching condition of Eq. (20b) must be obeyed by an ordinary polarized intense laser beam (ω_1, $\mathbf{k}_1$), its Rayleigh scattered light ($\omega_2 = \omega_1$, $\mathbf{k}_2$), and the extraordinary polarized second-harmonic light ($\omega_3 = -2\omega_1$, $\mathbf{k}_3$) which forms an elliptic cone around the incident beam. In a plane normal to the optic axis the cone angle φ_{cryst} between the second-harmonic light and the incident beam is defined by[39]

$$\cos\varphi_{\text{cryst}} = n_e(\lambda_1/2)/n_o(\lambda_1)\ . \tag{21}$$

Applying Snellius' law one obtains the respective angle φ_{air} outside the crystal. Since $n_e(\lambda_1/2)$ depends on the crystal stoichiometry, this angle can be regarded as a sensitive measure for the composition.[17] In Fig. 5 the computed cone angle φ_{air} is depicted as a function of the crystal composition for $\lambda_1 = 1064$ nm and $T = 24.5\,^{\circ}$C. The calculations agree well with our measurements and the result from Bates[39] measured at a slightly higher temperature.

The method of induced noncollinear frequency doubling (INCFD) uses two intense laser beams ($\mathbf{k}_1$, $\mathbf{k}_2$) which are crossed inside the crystal under an angle 2φ. Again the vectorial phase matching condition must be fulfilled, for example, by varying the temperature of the crystal and therefore the refractive indices. The INCFD method has the advantage that the interaction volume within the sample is limited in all three spatial directions. This allows one to perform a three-dimensional topographic inspection of the crystal by the measurement of the noncollinear phase matching temperature T^{INCFD} at any position in the crystal.[17] For a given experimental configuration (angle φ and fundamental wavelength λ_1) a calibration curve for the crystal composition as a function of T^{INCFD} can be derived from the generalized Sellmeier equation.[40]

2. Angle phase matching

The phase matching condition for type-I angle phase matching in $LiNbO_3$ can be written as

$$\frac{1}{n_o^2(\lambda_1)} = \frac{\cos^2\theta}{n_o^2(\lambda_1/2)} + \frac{\sin^2\theta}{n_e^2(\lambda_1/2)}\ , \tag{22}$$

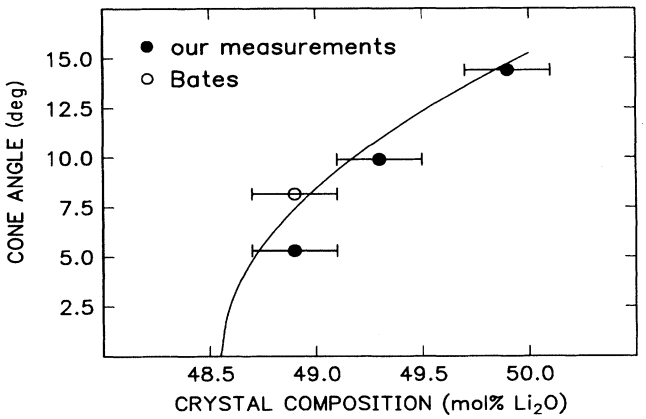

FIG. 5. Cone angle for spontaneous noncollinear frequency doubling as a function of the crystal composition. The curve is calculated from the generalized Sellmeier equation (see text). The angles are measured outside the crystal in a plane normal to the optic axis. The crystal composition for the literature value (Ref. 39) was determined by the Curie temperature and Eq. (1).

where θ denotes the direction of propagation in the crystal with respect to the optic axis. In Fig. 6 the phase matching angle is computed as a function of the crystal composition for $T = 24.5\,^{\circ}\mathrm{C}$ and two fundamental wavelengths. Our experimental data and the result from Hobden and Warner[35] are in good correspondence with the calculations.

The lower concentration limit of the calculated curves reveals the concentrations to be used for noncritically phase matched (phase matching angle 90°) frequency doubling for the respective wavelengths at room temperature. For 1152 nm and 1064 nm, e.g., we obtain 47.55 and 48.56 mol% Li_2O, respectively. A recently proposed equation for the 1064 nm phase matching temperature of $LiNbO_3$ as a function of the Li content[16] reveals 48.54 mol% Li_2O for $T_{PM} = 24.5\,^{\circ}\mathrm{C}$, which agrees excellently with our value.

3. *Phase matching temperature*

The phase matching condition for collinear noncritical type-I second-harmonic generation (SHG) is equivalent to

$$\Delta n_{SHG} = n_e(\lambda_1/2, T_{PM}) - n_o(\lambda_1, T_{PM}) = 0\,, \qquad (23)$$

which allows for a given Li content to compute the phase matching temperature T_{PM}. This is done for several fundamental wavelengths in Fig. 7. The experimental results of several other authors reveal good correspondence within an extremely wide temperature range from −160 to at least 400 °C.

Only in the Li-poor region for 1064 nm is there some disagreement between the results of two different authors.[15,16] Since the phase matching temperature changes in this region by about 200 °C within 0.2 mol% Li_2O in an extremely nonlinear manner, a slight difference in the composition may cause this discrepancy. This behavior of the phase matching temperature is due to the fact that the refractive indices at very low temperatures show only a weak temperature dependence, demanding therefore strong temperature changes to compensate for the composition change.

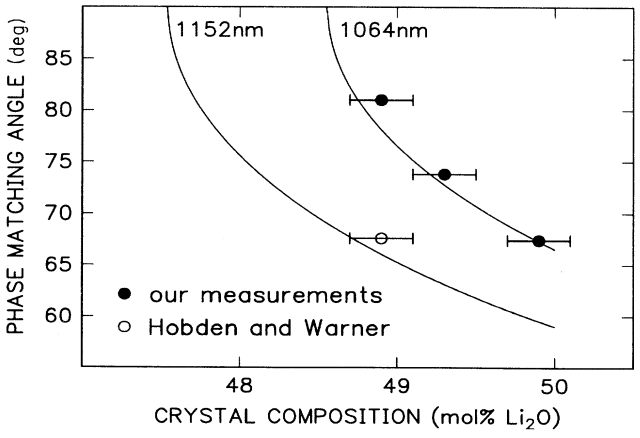

FIG. 6. Phase matching angle as a function of the crystal composition. The angles are measured inside the crystal with respect to the optic axis. The curves are calculated from the generalized Sellmeier equation (see text). The crystal composition for the literature value (Ref. 35) was obtained by the Curie temperature and Eq. (1).

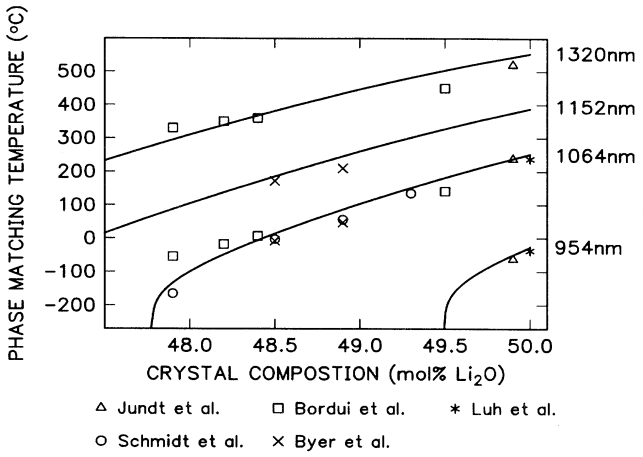

FIG. 7. Calculated phase matching temperature of $LiNbO_3$ as a function of the Li content in the crystal for various fundamental wavelengths. Data points are experimental values from several other authors (Refs. 8, 15, 16, 41, and 42). As far as necessary the crystal compositions were determined by an interpolation of the Curie temperature.

For high temperatures the calculated curve deviates from experimental results for at most 50 °C. This allows one to estimate the maximum error in our calculations of the refractive indices for high temperatures. With $\partial n_e/\partial T \approx 1 \times 10^{-4}/^{\circ}\mathrm{C}$ at 660 nm and 400 °C and a neglegible temperature variation of n_o(1320 nm) a maximum error of $\Delta n \approx 0.005$ can be stated. This is a rather good accuracy for this high-temperature region.

4. *Parametric oscillation and difference frequency mixing*

As a further test for our generalized Sellmeier equation, we calculated the phase matching temperatures for parametric oscillation in vapor transport equilibrated $LiNbO_3$ (49.9 mol% Li_2O). A comparison with the experimental results from Jundt *et al.*[8] is shown in Fig. 8. Edwards and Lawrence[18] measured the phase matching temperature for difference frequency generation in almost congruent $LiNbO_3$ (about 48.6 mol% Li_2O) for a pump wavelength of $\lambda_3 = 488$ nm. The comparison with our calculations in Fig. 8 for the respective experimental configuration reveals excellent correspondence also.

It should be mentioned that the calculations involve the refractive index for the idler wavelength which lies in the range between 2000 and 3000 nm. The good agreement shows that the generalized Sellmeier equation is an excellent description for the refractive indices even in this region.

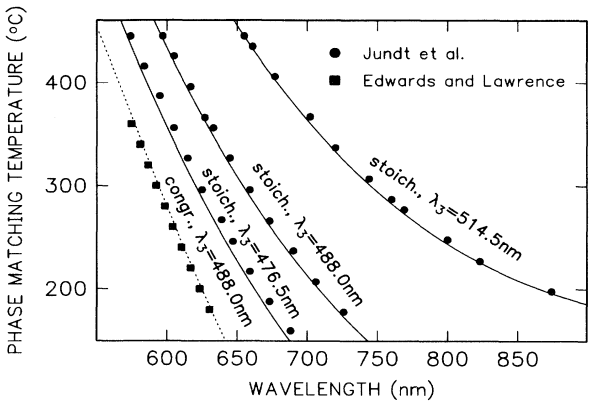

FIG. 8. Phase matching temperatures for difference frequency generation in congruent $LiNbO_3$ (dotted curve) and parametric oscillation in stoichiometric $LiNbO_3$ (solid lines) as a function of the signal wavelength. λ_3 denotes the pump wavelength. Data points correspond to experimental results from Edwards and Lawrence (Ref. 18) and Jundt *et al.* (Ref. 8).

D. Conclusion

We propose a generalized Sellmeier equation which describes the refractive indices of $LiNbO_3$ as a function of composition, wavelength, and temperature. The equation consists of two approximated oscillator terms for infrared and plasmonic contributions and two terms representing Nb on a Nb site and Li site. Only the latter two terms are composition and temperature dependent. The temperature variation is assumed to be proportional to the shift of the UV absorption edge with temperature. The parameters of this equation were fitted to our refractive index measurements and literature data. Calculations for a variety of effects in $LiNbO_3$ verify that the equation gives an accurate description of the refractive indices in the composition range from 47 to 50 mol % Li_2O, in the wavelength range from 400 to 1200 nm, and for temperatures between 50 and at least 600 K. The error in the calculated refractive indices is less than 0.001 for room temperature and less than 0.005 for higher temperatures. Extrapolations beyond these wavelength and temperature ranges still reveal good precision.

With this Sellmeier equation the parameters and calibration curves of all refractive-index-dependent characterization techniques for the stoichiometry of undoped $LiNbO_3$ can be derived. The phase matching conditions for nonlinear effects such as second-harmonic generation and parametric oscillation can be calculated with excellent accuracy.

ACKNOWLEDGMENTS

We are greatly indebted to B.C. Grabmaier for the growth and precise characterization of the sample crystals. We would also like to thank S.E. Kapphan who kindly furnished the VTE crystal. Financial support from the Deutsche Forschungsgemeinschaft (SFB 225) is gratefully acknowledged.

[1] R.J. Holmes and W.J. Minford, Ferroelectrics **75**, 63 (1987).
[2] H. Fay, W.J. Alford, and H.M. Dess, Appl. Phys. Lett. **12**, 89 (1968).
[3] I. Tomeno and S. Matsumura, J. Phys. Soc. Jpn. **56**, 163 (1987).
[4] P.F. Bordui, R.G. Norwood, C.D. Bird, and G.D. Calvert, J. Cryst. Growth **113**, 61 (1991).
[5] G.I. Malovichko, V.G. Grachev, and L.P. Yurchenko, Phys. Status Solidi **133**, K29 (1992).
[6] G.I. Malovichko *et al.*, Appl. Phys. A **56**, 103 (1993).
[7] R.L. Holman, Mater. Sci. Res. **11**, 343 (1978).
[8] D.H. Jundt, M.M. Feijer, and R.L. Byer, IEEE J. Quantum Electron. **QE-26**, 135 (1990).
[9] J.R. Carruthers, G.E. Peterson, and M. Grasso, J. Appl. Phys. **42**, 1846 (1971).
[10] I. Földváry, K. Polgár, R. Voszka, and R.N. Balasanyan, Cryst. Res. Technol. **19**, 1659 (1984).
[11] U. Schlarb *et al.*, Appl. Phys. A **56**, 311 (1993).
[12] K. Hofmann, Ph.D. thesis, TU München, 1987.
[13] L. Arizmendi, J. Appl. Phys. **64**, 4654 (1988).
[14] U. Olfen, R.A. Rupp, E. Krätzig, and B.C. Grabmaier, Ferroelectr. Lett. Sect. **10**, 133 (1989).
[15] N. Schmidt, K. Betzler, and B.C. Grabmaier, Appl. Phys. Lett. **58**, 34 (1991).
[16] P.F. Bordui, R.G. Norwood, D.H. Jundt, and M.M. Fejer, J. Appl. Phys. **71**, 875 (1992).
[17] A. Reichert and K. Betzler, Ferroelectrics **126**, 9 (1992).
[18] G.J. Edwards and M. Lawrence, Opt. Quantum Electron. **16**, 373 (1984).
[19] D.S. Smith, H.D. Riccius, and R.P. Edwin, Opt. Commun. **17**, 332 (1976).
[20] M.S. Shumate, Appl. Opt. **5**, 327 (1966).
[21] K. Betzler, A. Gröne, N. Schmidt, and P. Voigt, Rev. Sci. Instrum. **59**, 652 (1988).
[22] U. Schlarb and K. Betzler, Ferroelectrics **126**, 39 (1992).
[23] B.C. Grabmeier, W. Wersing, and W. Koestler, J. Cryst. Growth **110**, 339 (1991).
[24] N. Schmidt, K. Betzler, and S. Kapphan, Cryst. Lattice Defects Amorph. Mater. **15**, 103 (1987).
[25] N. Schmidt *et al.*, J. Appl. Phys. **65**, 1253 (1989).
[26] J.M. Stone, *Radiation and Optics* (McGraw-Hill, New York, 1963), p. 381.
[27] S.C. Abrahams and P. Marsh, Acta Crystallogr. B **42**, 61 (1986).
[28] E. Wiesendanger and G. Güntherodt, Solid State Commun. **14**, 303 (1974).
[29] D.M. Smyth, Ferroelectrics **50**, 419 (1983).
[30] A. Manoogian and J.C. Woolley, Can. J. Phys. **62**, 285 (1984).
[31] A. Manoogian and A. Leclerc, Phys. Status Solidi B **92**, K23 (1979).
[32] P.K. Gallagher, H.M. O'Bryan, E.M. Gyorgy, and J.T. Krause, Ferroelectrics **75**, 71 (1987).
[33] D. Redfield and W.J. Burke, J. Appl. Phys. **45**, 4566 (1974).

[34] A.M. Mamedov, Opt. Spektrosk. **56**, 1049 (1984) [Opt. Spectrosc. (USSR) **56**, 645 (1984)].
[35] M.V. Hobden and J. Warner, Phys. Lett. **22**, 243 (1966).
[36] U. Schlarb and K. Betzler, J. Appl. Phys. **73**, 3472 (1993).
[37] I. Földváry, K. Polgár, and A. Mecseki, Acta Phys. Hung. **55**, 321 (1984).
[38] J.A. Giordmaine, Phys. Rev. Lett. **8**, 19 (1962).
[39] H.E. Bates, J. Opt. Soc. Am. **61**, 904 (1971).
[40] U. Schlarb and K. Betzler (unpublished).
[41] Y.S. Luh, M.M. Fejer, R.L. Byer, and R.S. Feigelson, J. Cryst. Growth **85**, 264 (1987).
[42] R.L. Byer, J.F. Young, and R.S. Feigelson, J. Appl. Phys. **41**, 2320 (1970).